01 Jan 1968

Cell Model Of A Fluid. II. Thermodynamic Properties Of The System

Ralph G. Tross

Louis H. Lund
Missouri University of Science and Technology

Recommended Citation

R. G. Tross and L. H. Lund, "Cell Model Of A Fluid. II. Thermodynamic Properties Of The System," *Journal of Mathematical Physics*, vol. 9, no. 11, pp. 1957 - 1975, American Institute of Physics, Jan 1968.
The definitive version is available at https://doi.org/10.1063/1.1664531

RESEARCH ARTICLE | OCTOBER 28 2003

Cell Model of a Fluid. II. Thermodynamic Properties of the System

Ralph G. Tross; Louis H. Lund

J. Math. Phys. 9, 1957–1975 (1968)
https://doi.org/10.1063/1.1664531

JOURNAL OF MATHEMATICAL PHYSICS VOLUME 9, NUMBER 11 NOVEMBER 1968

Cell Model of a Fluid. II. Thermodynamic Properties of the System

RALPH G. TROSS*† AND LOUIS H. LUND
University of Missouri at Rolla, Rolla, Missouri

(Received 3 May 1968)

In Paper I of this series (preceding paper) the model was formulated mathematically and the solution derived in the form of an infinite series. The convergence and analyticity of the solution were investigated. It was then applied to one-, two-, and three-dimensional systems with nearest-neighbor interactions, and low-temperature series for these systems were obtained. In the present article the thermodynamics of the model are investigated. The series solution of the partition function derived in Paper I is applied to systems with interaction potentials of increasing complexity. The validity of the model is established by showing that in the appropriate limits it leads correctly to the ideal gas and the Tonks equation of state. It is shown that the model is capable of portraying phase transitions and gives realistic results thermodynamically. Finally various finite one-, two-, and three-dimensional systems are analyzed numerically by high-speed computer and their thermodynamic properties and pair-correlation functions are examined. Interesting conclusions emerge concerning the range of order in such systems and the probable critical temperatures.

I. INTRODUCTION

In the first[1] of this series of two articles, a one-dimensional fluid was examined, in which every particle interacts with every other one with a modified Lennard–Jones-type potential. The system was cast in the mold of a cell model which could be treated by means of the Ising formalism. We derived the partition function for such a system, showed how the partition function for two- and three-dimensional systems with a limited number of bonds per particle could be derived from the one-dimensional one and found a solution to the problem in the form of an infinite series. This series was shown to be absolutely convergent and proved convenient for investigating the analyticity of the system. The analysis confirmed the results previously obtained by Yang and Lee.[2] It was seen in I that the series could be summed for a one-dimensional system with nearest-neighbor interactions and that the resultant closed-form solution agreed with that obtainable by matrix methods. This served to establish the validity of the model in that limit. In addition, the corresponding low-temperature series for two- and three-dimensional systems with nearest-neighbor interactions were readily obtained from the one-dimensional series. Thus it proved possible to calculate series expansions in all dimensions by identical algebraic techniques.

In this article we shall investigate the thermodynamic behavior of this fluid model. First, certain potentials will be considered for which the system can be analyzed in the thermodynamic limit. If there is no interaction of any kind, we shall find that the model leads correctly to the equation of state of an ideal gas. If the hard repulsive core is retained, the fluid obeys the well-known Tonks equation of state.[3] Next a system with hard-rod repulsive and nearest-neighbor attractive interactions is examined. It has the advantage that one can write the equation of state in closed form. Aside from the absence of a phase transition the system exhibits interesting and quite realistic thermodynamic properties and has the advantage of being very tractable mathematically. Another potential which allows one to proceed to the thermodynamic limit is one in which the range parameter γ is allowed to go to zero, resulting in an infinitely long-range interaction. While this does not correspond to any real fluid, it is an interesting limit mathematically. One can show rigorously, as we shall see, that such a system exhibits phase transitions at all finite temperatures.

Although it has not been possible thus far to go to the thermodynamic limit in systems interacting with the general Lennard–Jones potential,[1] the series solution of the partition function, Eq. (4.7) of Paper I, is well suited for numerical analysis by high-speed computer. Accordingly one-, two-, and three-dimensional systems of finite size are analyzed and their thermodynamic properties determined. The results are surprisingly realistic. Although no true phase transition is encountered, as one would expect for systems of finite size, there are a number of indications that such a transition may occur in the thermodynamic limit. The most convincing of these are the conclusions on long-range order that emerge from a study of the pair-correlation functions of the system.

* Based upon a dissertation submitted to the Graduate Faculty of the University of Missouri at Rolla in partial fulfillment of the requirements for the Ph.D. degree. Work supported in part by a NASA Predoctoral Traineeship and an NSF post-doctoral grant.

† Present address: Dept. of Math., University of Ottawa, Ottawa, Canada.

[1] R. G. Tross and L. H. Lund, J. Math. Phys. **9**, 1940 (1968), hereafter referred to simply as I or Paper I.

[2] C. N. Yang and T. D. Lee, Phys. Rev. **87**, 404, 410 (1952).

[3] L. Tonks, Phys. Rev. **50**, 955 (1936).

The point of departure for the analysis in this article is the model developed in I and the series form of the partition function in Eq. (4.7)

$$
\begin{aligned}
&Q_N = 2C_N \sum_{n=0}^{[N/2]} T_n; \quad C_N = \exp(N\nu) \\
&T_n = \cosh[(N-2n)\nu] X^{-n/2} t_n (1 - \tfrac{1}{2}\delta_{n,N/2}) \\
&t_n = \left(\frac{1}{n!}\right) \sum_{q_1=1}^{N}{}' \cdots \sum_{q_n=1}^{N}{}' \prod_{r=1}^{n} \prod_{\substack{s=1 \\ (r<s)}}^{n} x_{q_r - q_s} \\
&x_r = \exp\{8\theta_r\}; \quad X = \prod_{r=1}^{N} x_r \\
&\theta_r = -(\tfrac{1}{4})\beta\phi_r; \quad \phi_r = (\tfrac{1}{2})(V_r + V_{N-r}) \\
&V_r = -\zeta / r^{\gamma} \\
&\beta = 1/kT; \quad e^{2\nu} = (l/\lambda) \exp\left\{\beta\left(g - \sum_{r=1}^{N} \phi_r\right)\right\},
\end{aligned}
\tag{1.1}
$$

where ζ defines the depth of the potential cell and γ is a range parameter. (For further definitions see Paper I.)

II. THERMODYNAMICS OF INFINITE SYSTEMS

In this section we investigate the thermodynamic behavior of certain infinite systems, i.e., systems which are infinite in the sense that the solution holds in the thermodynamic limit, $N \to \infty$, where N is the total number of cells in the system. This limit implies that either the cell parameter $l = L/N$ goes to zero (L being the length of the one-dimensional system) or the length of the system becomes infinite. These two limits are not equivalent as we shall see.

A. Ideal Gas

We wish first to check the validity of the model in the ideal-gas limit and assume the interaction potential to be $V_r = 0$. This potential does not, however, eliminate the hard-core repulsive interaction which was built into the model by our choice of cell parameter and the introduction of an exclusion principle. We neglect this point for the moment and come back to it later. The series, Eq. (1.1), now takes the form

$$
\begin{aligned}
Q_N &= 2\exp(N\nu) \sum_{n=0}^{[N/2]} \binom{N}{n} \\
&\quad \times \cosh[(N-2n)\nu](1 - \tfrac{1}{2}\delta_{n,N/2}) \\
&= \sum_{n=0}^{N} \binom{N}{n} \exp(2n\nu) = \left(1 + \frac{V\xi}{\lambda N}\right)^N,
\end{aligned}
\tag{2.1}
$$

where we have used the obvious identity

$$
t_n = \left(\frac{1}{n!}\right) \sum_{q_1=1}^{N}{}' \cdots \sum_{q_n=1}^{N}{}' 1 = \binom{N}{n}.
$$

In Eq. (2.1), V is the "volume" of the system. For the basic one-dimensional fluid the volume is, of course, the length of the line L. However, since there is no attractive interaction among the particles, we may assume the cell to be a tiny square of dimensions $l \times l$ or cube of dimensions $l \times l \times l$. The string of squares or cubes can then be wrapped around a torus as in Sec. 2B of I to generate a two- or three-dimensional system. For higher-dimensional systems we must, of course, redefine λ in an appropriate way. [We must then use the following definition: $\lambda = (\beta h^2/2\pi m)^{d/2}$, where d is the dimension of the system. This follows directly from integrating the kinetic part of the partition function.]

The hard-core repulsive potential can now be eliminated in going to the thermodynamic limit. To do so, we let the cell parameter l shrink to zero while $N \to \infty$, i.e., we keep the volume V fixed. Then

$$
Q = \lim_{N\to\infty} Q_N = \exp(V\xi/\lambda) = \exp(\beta p V). \tag{2.2}
$$

We have then that $\ln Q = \beta p V = V\xi/\lambda$. From the well-known relation $\langle n \rangle = \xi[\partial/\partial\xi(\ln Q)]_\beta$ we then obtain the equation of state of an ideal gas[4,5]

$$
\beta p V = \langle n \rangle, \tag{2.3}
$$

where $\langle\ \rangle$ designates an ensemble average or expectation value. It should be observed once more that in obtaining this equation of state from our model we were obliged to let the particles shrink to ideal points in order to eliminate the built-in repulsive potential.

B. A Fluid of Hard Rods

We next consider a fluid of hard rods, i.e., a system of particles with a hard repulsive core and no attractive interaction. The partition function, before we go to the thermodynamic limit, is then the same as that in Eq. (2.1), i.e., $Q_N = (1 + l\xi/\lambda)^N$. The hard repulsive core has, of course, not been eliminated. In order to retain the repulsive potential, we must go to the limit in a different way: we keep l, the cell parameter, fixed while we let $N \to \infty$. This is tantamount to letting the volume go to infinity. For the density of the system we obtain

$$
\rho = \xi[\partial/\partial\xi(1/N) \ln(Q_N)]_\beta = (l\xi/\lambda)/(1 + l\xi/\lambda). \tag{2.4}
$$

Here $\rho = \langle n \rangle / N$ is a dimensionless density. [This density is related to the usual density as follows: $\rho = \langle n \rangle / N = l/v$. If m_0 is the mass per particle, then $\tilde{\rho} = m_0(1/v) = m_0\rho/l$ is the density as usually

[4] K. Huang, *Statistical Mechanics* (John Wiley & Sons, Inc., New York, 1963).

[5] D. ter Haar, *Elements of Statistical Mechanics* (Holt, Rinehart, and Winston, Inc., New York, 1964).

defined.] One can also think of ρ as the proportion of the line occupied by particles, for we can write $\rho = \langle n\rangle l/Nl = L_0/L$, where L_0 is the length which the particles would occupy if they were tightly packed. Using (2.4) and keeping the cell parameter l fixed, one can now go to the thermodynamic limit and obtain:

$$\beta pL = \lim_{N\to\infty} \ln (Q_N) = \langle n\rangle/(1 - \rho) \qquad (2.5)$$

or

$$pL(1 - \rho) = pL_{\text{eff}} = \langle n\rangle KT$$

which is the well-known Tonks equation of state,[3] with $L_{\text{eff}} = L(1 - \rho)$ denoting the net length of the line not occupied by particles, i.e., the free "volume" of the system. (We use the symbol p to represent the "pressure" of the system in the appropriate units. Thus, in a one-dimensional system pressure has the units of force.)

By identical arguments to those given in the preceding section one sees that the analysis holds for systems of all dimensions and that consequently L and L_{eff} can be replaced by V and V_{eff}, respectively. Thus the model yields the correct equations of state for a fluid of hard rods, hard disks, or hard spheres.

One can show in this connection the effect of the hard-core potential on the series solution of Eq. (1.1) and on the choice of the cell parameter l. This is done in Appendix A.

C. One-Dimensional Fluid with Nearest-Neighbor Interactions

We examine in this section the thermodynamic properties of a one-dimensional fluid comprised of particles with hard-core repulsive potential and nearest-neighbor attractive interactions. While such a fluid is of very limited practical interest, it has the advantage of being mathematically tractable since the equation of state can be written in closed form. Furthermore, there are many striking parallels with real fluids, although such a system cannot have a phase transition, as we know from Van Hove's work.[6]

It was shown in I (Sec. 6A) that the partition function of this fluid is given by

$$Q_N = C_N \cosh^N (\nu) \times \{[1 + (1 + \omega)^{\frac{1}{2}}]^N + [1 - (1 + \omega)^{\frac{1}{2}}]^N\}, \qquad (2.6)$$

where $C_N = \exp(N\nu)$ and $\omega = (x_1^{-1} - 1)\,\text{sech}^2\,\nu$. In the thermodynamic limit we obtain for the grand potential[5]

$$q = \beta pl = \lim_{N\to\infty} 1/N \ln (Q_N) = \nu + \ln(\cosh\nu) + \ln[1 + (1 + \omega)^{\frac{1}{2}}]. \qquad (2.7)$$

[6] L. Van Hove, Physica **16**, 137 (1950).

TABLE I. Relationship between density ρ, Gibbs free energy g, and parameter ν.

ρ	0	$\frac{1}{2}$	1
g	$-\infty$	$1/\beta \ln(\lambda x_1^{-1}/l)$	$+\infty$
ν	$-\infty$	0	$+\infty$

The density is then

$$\rho = \langle n\rangle/N = \xi(\partial q/\partial\xi)_\beta = (\tfrac{1}{2})(\partial q/\partial\nu)_\beta = (\tfrac{1}{2})[1 + \tanh\nu/(1 + \omega)^{\frac{1}{2}}]. \qquad (2.8)$$

While ν is a function of the temperature, interaction potential, and Gibbs free energy [cf. Eq. (1.1)], we can in fact consider it a free parameter in Eqs. (2.7) and (2.8) so that these two equations give the equation of state parametrically. Table I gives the relationship between ρ, g, and ν. Pressure–density data computed from these two equations are plotted in Figs. 1 and 2. (Actually $q = \beta p l$ is plotted vs ρ. For a given isotherm this is, of course, proportional to p.) The graphs show clearly that the pressure of the system is reduced by a decrease in the temperature or by an increase in the strength of the interaction potential. We wish next to compute the isothermal compressibility. This is given by

$$K_T = -(1/v)(\partial v/\partial p)_\beta = (1/\rho)(\partial\rho/\partial p)_\beta = (\beta l/2\rho^2)(\partial\rho/\partial\nu)_\beta = (\beta l x_1^{-1}\,\text{sech}^2\,\nu)/[\rho^2(1 + \omega)^{\frac{3}{2}}]. \qquad (2.9)$$

Figures 3 and 4 are plots of compressibility vs density corresponding to the p–ρ plots in Figs. 1 and 2, respectively. The behavior is physically reasonable: compressibility increases with decreasing temperature and increasing strength of the interaction. This parameter is, of course, of interest because of its relation to the slope of the p–ρ curve [cf. Eq. (2.9)] and its well-known connection with fluctuations in the number of particles of the system. The compressibility is therefore a valuable indicator of a change in phase and one expects the compressibility curve to have a discontinuity at the critical density. No such behavior is apparent in these two figures in consonance with Van Hove's theorem.[6]

The internal energy density of the system is determined as follows:

$$u = \langle H\rangle/N = -(\partial q/\partial\beta)_\xi = -[(\partial q/\partial\nu)_\beta(\partial\nu/\partial\beta)_\xi + (\partial q/\partial\beta)_\nu] = -2\rho(\partial\nu/\partial\beta)_\xi + (\partial q/\partial\beta)_\nu = (\tfrac{1}{2})\rho kT - (\zeta/2) \times \{2\rho - [x_1^{-1}\,\text{sech}^2\,\nu]/[1 + \omega + (1 + \omega)^{\frac{1}{2}}]\}. \qquad (2.10)$$

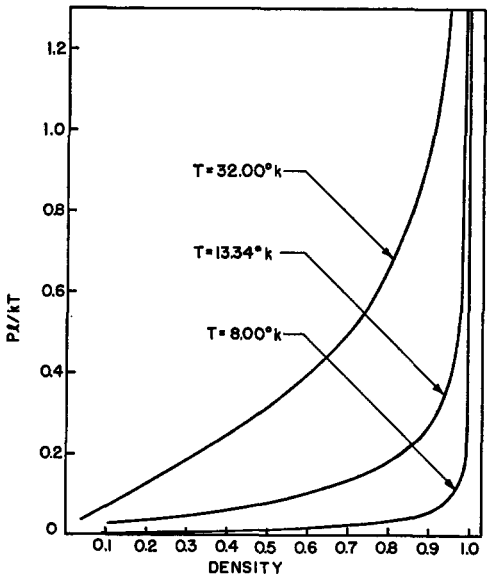

FIG. 1. Pressure-vs-density isotherms for a one-dimensional system with nearest-neighbor interactions; $\zeta = 64k$.

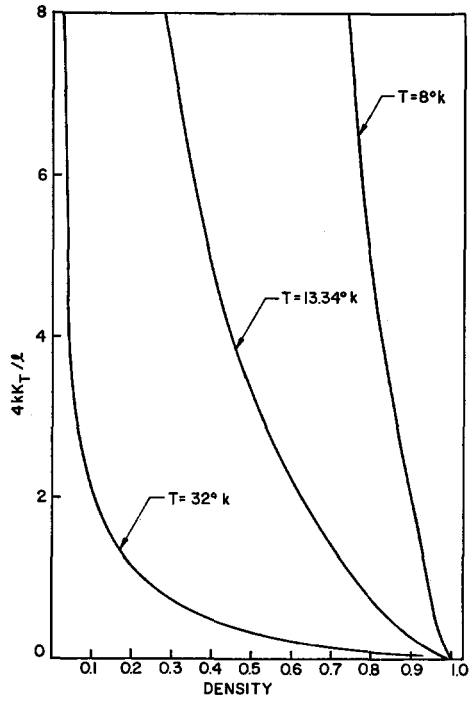

FIG. 3. Compressibility vs density for a one-dimensional system with nearest-neighbor interactions; $\zeta = 64k$, various temperatures.

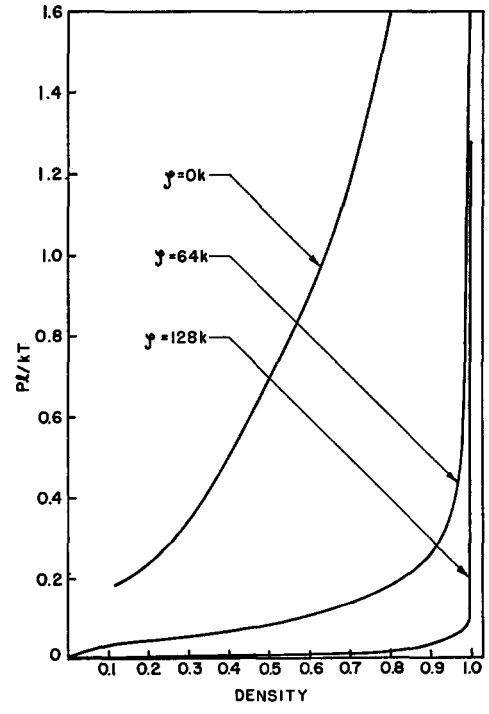

FIG. 2. Pressure-vs-density curves for various potential-well depths for a one-dimensional system with nearest-neighbor interactions; $T = 13.34°K$.

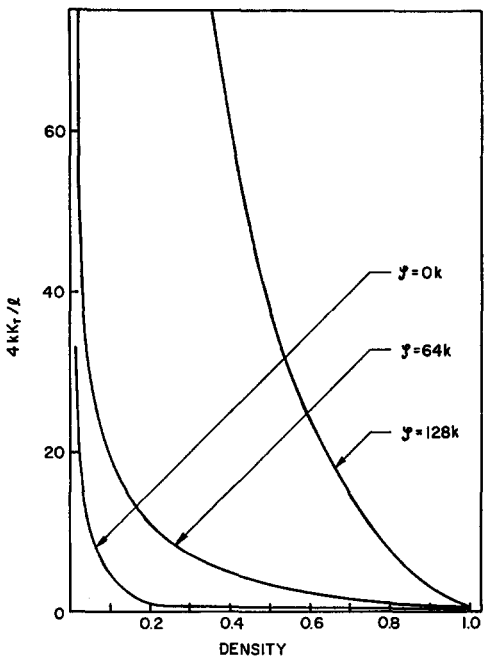

FIG. 4. Compressibility vs density for a one-dimensional system with nearest-neighbor interactions; $T = 13.34°K$; various potential-well depths.

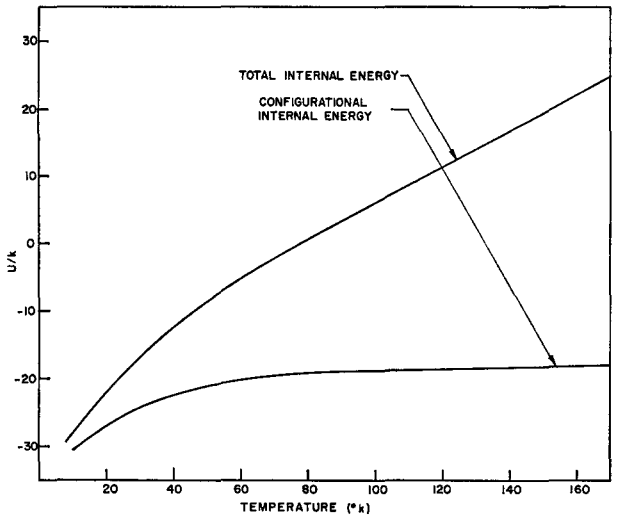

FIG. 5. Internal energy density vs temperature for a one-dimensional system with nearest-neighbor interactions.

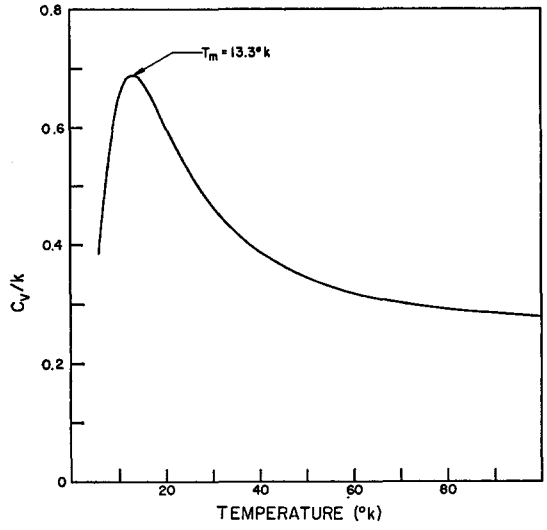

FIG. 6. Specific heat vs temperature for a one-dimensional system with nearest-neighbor interactions; $\rho = \frac{1}{2}$.

Energy density is plotted vs temperature in Fig. 5 for $\rho = \frac{1}{2}$. One can readily check the validity and meaning of the various terms in (2.10) by proceeding directly from the partition function. This analysis is carried out in Appendix B. It is apparent from (2.10) that the zero-point energy density of the system is $u = -\zeta\rho$, which corresponds to a zero-point energy per particle of $-\zeta$ and thus accords with physical intuition.

From (2.10) one can compute the specific heat of the system as follows:

$$C_v = (\partial u/\partial T)_v = -k\beta^2(\partial u/\partial\beta)_\rho$$
$$= (\tfrac{1}{2})k\rho + (\tfrac{1}{4})k(\beta\zeta)^2 x_1^{-1}$$
$$\times \operatorname{sech}^4 \nu/[(1+\omega)^{\frac{1}{2}}(1+(1+\omega)^{\frac{1}{2}})^2]. \quad (2.11)$$

As is well-known, the interest in the specific heat arises from the obvious connection between it and the fluctuations in energy of the system. One expects these to be very large in the critical region so that the specific heat is a valuable indicator of phase changes. In the critical region, (2.11) reduces to

$$C_v(\rho = \tfrac{1}{2}) = k/4 + k\epsilon^2 \operatorname{sech}^2 \epsilon, \quad (2.12)$$

where $\epsilon = (\frac{1}{4})\beta\zeta$. Figure 6 is a plot of this relation. While the maximum at $T_m = 0.208\zeta/k$ obviously represents large fluctuations in density, it does not correspond to a phase transition. If we let $\eta = 2kT/\zeta$, we can recast (2.12) in the form

$$(C_v - k/4) = k\eta^{-2}\exp(-1/\eta)$$
$$\times \sum_{r=0}^{\infty}(-1)^{r+1} r \exp[-(r-1)/\eta]$$
$$\doteq k\eta^{-2}\exp[-1/\eta] \quad (\eta \ll 1), \quad (2.13)$$

which shows that the configurational specific heat approaches zero exponentially as $T \to 0$, i.e., faster than the T^3 law of Debye.[7]

It is possible to eliminate the parameter ν in the equation of state and to write the pressure as an explicit function of the density. One obtains then from Eqs. (2.7) and (2.8):

$$pl(1-\rho) = kTx_1^{-1}$$
$$\times \{(\rho - \tfrac{1}{2}) + [(\rho - \tfrac{1}{2})^2 + x_1\rho(1-\rho)]^{\frac{1}{2}}\}. \quad (2.14)$$

One may notice in passing that for $x_1 \to 1$ this merges into the correct equation of state for the Tonks fluid. One can rewrite (2.14) in a somewhat more suggestive way:

$$pl_{\text{eff}} = kT\rho_{\text{eff}}, \quad (2.15)$$

where $l_{\text{eff}} = l(1-\rho) = (1/N)L(1-\rho) = (1/N)L_{\text{eff}}$ [cf. Eq. (2.5)] and $\rho_{\text{eff}} = (\rho - \frac{1}{2}) + [(\rho - \frac{1}{2})^2 + x_1\rho(1-\rho)]^{\frac{1}{2}}$. l_{eff} thus represents an effective cell parameter related to the effective or free "volume" by the relation $l_{\text{eff}} = \lim_{N\to\infty}\{(L - L_0)/N\}$. Similarly ρ_{eff} represents an effective density which, by virtue of the interaction potential, is lower than the true density. The pressure of the system is thus reduced by the interaction as we saw in Fig. 2. One can also cast the equation of state in the form of a van der Waals equation

$$(p + a)(L - b) = \langle n\rangle kT \quad (2.16)$$

where

$$a = p\{x_1/[(1 - L/2L_0) + (1 - L/2L_0)^2$$
$$+ x_1(L/L_0 - 1)] - 1\}$$

[7] J. M. Ziman, *Principles of the Theory of Solids* (Cambridge University Press, Cambridge, England, 1964).

and

$$b = L\rho = \langle n \rangle l = L_0.$$

The effect of the hard-core repulsion is contained in b, while a reflects the effect of the attractive potential. It is readily shown that $a \geq 0$. This form of the equation of state lends itself to a virial expansion which yields

$$p = \rho kT[1 + (2 - x_1)\rho + (4 - 5x_1 + 2x_1^2)\rho^2 + (8 - 18x_1 + 16x_1^2 - 5x_1^3)\rho^3 + (16 - 56x_1 + 82x_1^2 - 55x_1^3 + 14x_1^4)\rho^4 + (32 - 160x_1 + 340x_1^2 - 365x_1^3 + 196x_1^4 - 42x_1^5)\rho^5 + \cdots]. \quad (2.17)$$

Figure 7 is a plot of the second virial coefficient obtained from this expansion and of the true virial coefficient for a three-dimensional fluid. The similarity of these curves is rather surprising; their limit as $T \to \infty$, however, is different. From (2.14) it is possible to compute all thermodynamic functions in nonparametric form. Only a few results will be given here. For the internal energy density one finds, for example,

$$u = (\tfrac{1}{2})\rho kT - \rho\zeta\{1 - 2(1 - \rho)/[1 + 2((\rho - \tfrac{1}{2})^2 + x_1\rho(1 - \rho))^{\frac{1}{2}}]\}, \quad (2.18)$$

while the specific heat is given by

$$C_v = (\tfrac{1}{2})k\rho + 2k(\beta\zeta)^2\{\rho(1 - \rho)/[1 + 2((\rho - \tfrac{1}{2})^2 + x_1\rho(1 - \rho))^{\frac{1}{2}}]\}^2\{x_1/[(\rho - \tfrac{1}{2})^2 + x_1\rho(1 - \rho)]^{\frac{1}{2}}\}, \quad (2.19)$$

which for $\rho = \frac{1}{2}$ reduces again to expression (2.12). The chemical potential per particle is

$$g = kT \ln(\lambda/l) + 2kT \ln\{\rho_{\text{eff}}/[x_1(\rho(1 - \rho))^{\frac{1}{2}}]\}, \quad (2.20)$$

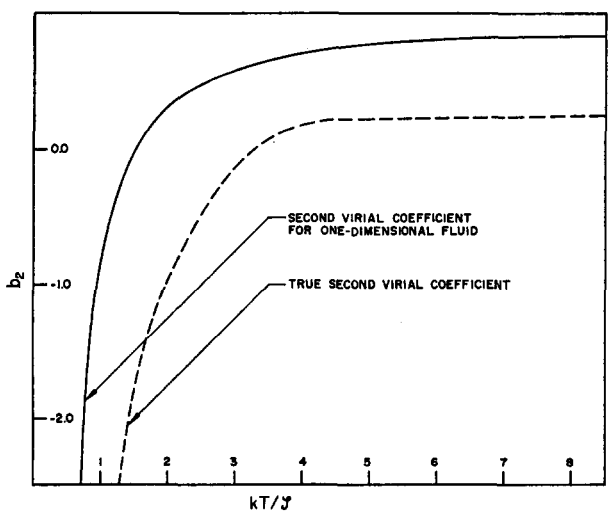

FIG. 7. Second virial coefficient vs temperature for a one-dimensional fluid with nearest-neighbor interactions.

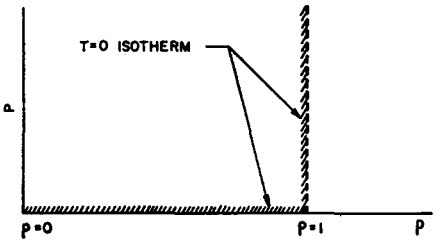

FIG. 8. Degenerate phase transition of the one-dimensional fluid with nearest-neighbor interactions.

where ρ_{eff} is given by (2.15). Other functions are readily determined from (2.14) but are not included here.

Before leaving this system we observe from (2.14) that $p = 0$ at $T = 0$ for all values of the density except $\rho = 1$. For the latter density we find

$$\lim_{\substack{T\to 0 \\ \rho\to 1}} p = \lim_{\substack{T\to 0 \\ g\to\infty}} (kT/l)[\tfrac{1}{2} \ln T + \zeta/kT + g/kT] + \text{finite terms} = +\infty. \quad (2.21)$$

Thus at $T = 0$ this system experiences a degenerate phase transition as shown in Fig. 8. One can also arrive at this conclusion by considering the analyticity of the partition function. One finds then that the zeros of the partition function of this fluid, just like those of the corresponding one-dimensional Ising ferromagnet, are distributed on the unit circle in the complex y plane.[8] These zeros cannot approach the real axis closer than $\alpha_{\min} = 2\cos^{-1}[(1 - x_1^{-1})^{\frac{1}{2}}]$. Hence[2] a phase transition can occur only as $T \to 0$ or $x_1 \to \infty$, and these transitions are degenerate.

D. A Fluid with Infinite-Range Interactions

We shall consider next a fluid with an attractive potential of infinitely long range, i.e., a potential where the range parameter γ goes to zero [cf. Eq. (1.1)]. A comparable magnetic potential in which all exchange interactions are identical has been applied by Kittel and Shore to a Heisenberg ferromagnet.[9] For a fluid such a potential has no physical counterpart; however, it constitutes an interesting limiting case to systems with interaction potentials of increasingly longer range. An alternative point of view is also possible. It was shown in I that, in considering systems with nearest-neighbor interactions, the coordination number increases as the dimension of the system is increased. The system considered here could therefore be thought of as a limiting case to a sequence of

[8] T. L. Hill, *Statistical Mechanics* (McGraw-Hill Book Co., Inc., New York, 1956).

[9] C. Kittel and H. Shore, Phys. Rev. **138**, 1165 (1965).

nearest-neighbor systems of increasingly higher dimensionality. Specifically, then, the potential we wish to examine is

$$V_s = \begin{cases} 0 & (s = 0) \\ -\zeta & (s \neq 0) \end{cases} \quad \text{(Mod. } N\text{)}. \qquad (2.22)$$

If we substitute this potential in the partition function, Eq. (1.1), we find that

$$t_n = (1/n!) \sum_{q_1=1}^{N}{}' \cdots \sum_{q_n=1}^{N}{}' \exp\left(2 \sum_{\substack{r=1 \\ (r<s)}}^{n} \sum_{s=1}^{n} \beta\zeta\right)$$

$$= \binom{N}{n} \exp\,[n(n-1)\beta\zeta]. \qquad (2.23)$$

Consequently the partition function takes the form

$$Q_N = C_N \sum_{n=0}^{N} \binom{N}{n} x^{-n(N-n)} \cosh\,[(N-2n)v] \qquad (2.24)$$

or

$$Q_N = \sum_{n=0}^{N} \binom{N}{n} y^n x^{-n(N-n)},$$

where $y = \exp(2v)$, $C_N = \exp(Nv)$, and $x = \exp(\beta\zeta)$. The sum in (2.24), although suggestive, is not readily evaluated. It is suited, however, to numerical evaluation and theoretical analysis. We present some numerical results first. For the density one obtains

$$\rho = (\tfrac{1}{2})(\partial q/\partial v)_\beta = (\tfrac{1}{2})(1 + T_v/NT), \qquad (2.25)$$

where

$$T(v, x) = \sum_{n=0}^{N} \binom{N}{n} x^{-n(N-n)} \cosh\,[(N-2n)v]$$

and

$$T_v = (\partial T/\partial v)_x.$$

For the compressibility we find:

$$K_T = (\beta l/4\rho^2)[T_{vv}/NT - (2\rho - 1)^2 N], \qquad (2.26)$$

where $T_{vv} = (\partial^2 T/\partial v^2)_x$. The internal energy density is

$$u = (\tfrac{1}{2})\rho kT - \zeta[(N-1)\rho - (T_x/NT)], \qquad (2.27)$$

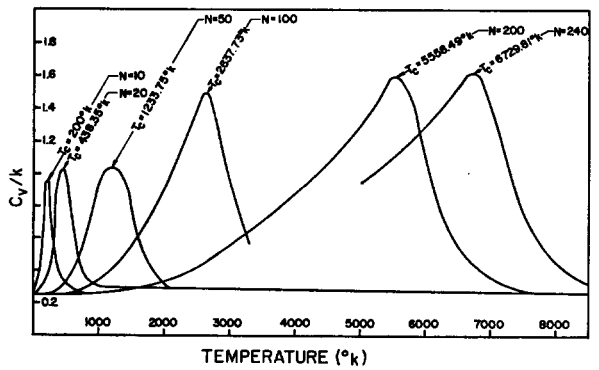

FIG. 9. Specific heat vs temperature for a one-dimensional system with infinite-range interactions; $\rho = \frac{1}{2}$.

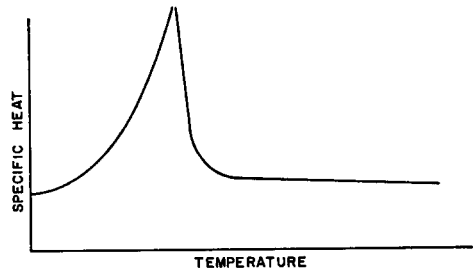

FIG. 10. Typical experimental specific-heat curve. (See Refs. 10 and 11.)

where $T_x = (\partial T/\partial x)_v$. Finally, the specific heat is

$$C_v = (\tfrac{1}{2})k\rho + k(\beta\zeta)^2 \times \{(1/NT)[(2\rho - 1)NT_x - T_{xv}]^2/[(2\rho - 1) \times NT_v - T_{vv}] + (1/NT^2)(TT_{xx} - T_x^2)\}, \qquad (2.28)$$

where $T_{xv} = (\partial^2 T/\partial x \partial v)$ and $T_{vv} = (\partial^2 T/\partial v^2)_x$.

Figure 9 is a plot of specific heat vs temperature for systems ranging in size from 10 to 240 cells and for a density of $\rho = \frac{1}{2}$. It appears from the graphs that the maxima tend to some sort of a limit, although it is not clear what this limit is. However, inspection of the data in Table II suggests that the quantity $N\zeta\beta_m$

TABLE II. Tabulated data on the maxima of the specific heat curves in Fig. 9.

System size (N)	Temperature of specific-heat maxima (T_m)	$N\zeta\beta_m$
10	193.95	3.30
20	438.35	2.92
50	1233.76	2.69
100	2637.53	2.43
200	5558.49	2.30
240	6729.81	2.28

approaches a limit 2.0. The analysis which follows at the end of this section shows that this is in fact the correct limit. One also observes from Fig. 9 that the specific heat curves assume a characteristic shape. A typical experimental specific-heat curve is shown in Fig. 10. It is based on the curves obtained by Nix and Shockley for alloys exhibiting typical order–disorder phase transitions.[10] A similar specific heat curve for xenon was published recently by Edwards, Lipa, and Buckingham.[11] It is quite apparent that the curves in Fig. 9 approach the characteristic shape of the experimental curves. Pressure–density curves are

[10] F. C. Nix and W. Shockley, Rev. Mod. Phys. **10**, 1 (1938).
[11] C. Edwards, J. A. Lipa, and M. J. Buckingham, Phys. Rev. Letters **20**, 496 (1968).

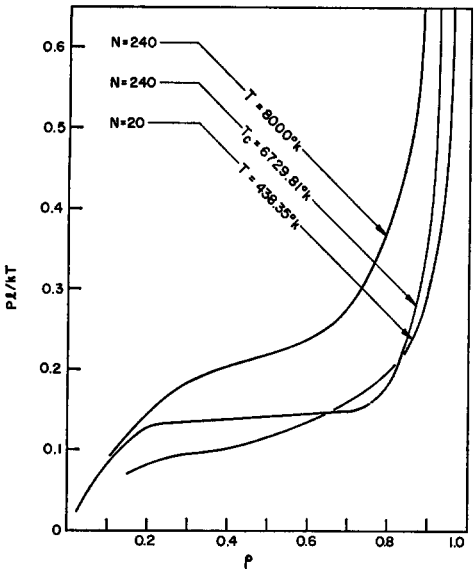

FIG. 11. Pressure-vs-density isotherms of one-dimensional systems with infinite-range interactions.

presented in Fig. 11. It is obvious that the isotherm of the 240-cell system at its "critical" temperature (i.e., the temperature where the specific heat curve has a maximum) is very nearly that of a system undergoing a phase transition. Conversely, the 8000°K isotherm, which is well above the "critical" temperature for this system, shows no such behavior. For comparison the

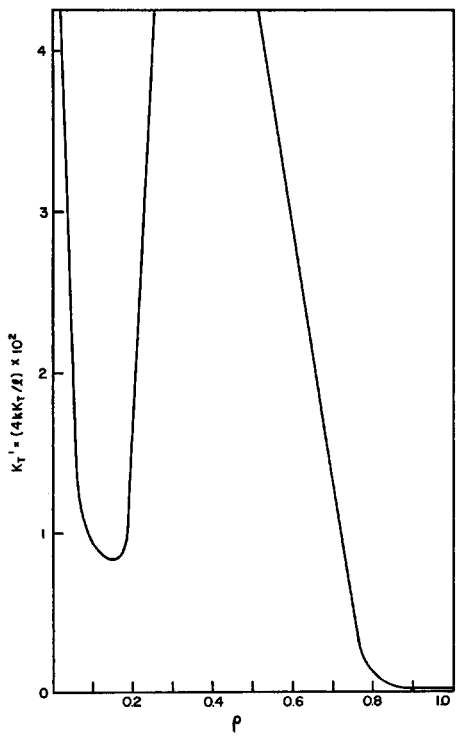

FIG. 12. Compressibility-vs-density curve for a one-dimensional system of 240 cells with infinite-range interactions.

"critical" isotherm for a very much smaller system also gives no indication of any phase change. "Critical" isotherms for systems of intermediate size (not shown to avoid confusion) gradually approach a phase transition with increasing system size.

A compressibility-vs-density plot for the 240-cell system at its "critical" temperature appears in Fig. 12. The compressibility curve very clearly approaches a discontinuity which is in keeping with the nearly horizontal isotherm in Fig. 11. Since the system is finite there is, of course, no true discontinuity, but the maximum value of the K_T curve cannot be determined from the computer data.

Figures 11 and 12 show quite convincingly that the system approaches a change of phase. It is possible to generalize and confirm the numerical results by analyzing Eq. (2.24). Suppose that T_m is the maximum term in the partition function, then clearly

$$q = \lim_{N\to\infty} (1/N) \ln (Q_N) = \nu + \lim_{N\to\infty} (1/N) \ln (T_m) + R. \tag{2.29}$$

Here

$$R = \lim_{N\to\infty} (1/N) \ln \left(1 + \sum_n T_n/T_m\right) = 0,$$

since there are N terms appearing in the argument of the logarithm, and $|T_n/T_m| < 1$ so that

$$|R| < \lim_{N\to\infty} (1/N) \ln N = 0.$$

In the thermodynamic limit we can thus determine all thermodynamic functions from the maximum term, T_m. Since we are interested in phase transitions, furthermore, it suffices to examine the case $\rho = \frac{1}{2}$, i.e., $\nu = 0$. To find the maximum term in the sum

$$T_n(x, 0) = \sum_{n=0}^{N} \binom{N}{n} x^{-n(N-n)}$$

we observe that the summand can be written as an exponential by means of the Stirling approximation. Noting that the summand attains a maximum as the exponent does, we obtain the following condition:

$$\ln (N/n - 1) + (2n - N)\beta\zeta = 0. \tag{2.30}$$

Letting $n/N = \rho$ as before [where we have used (2.29)] this leads to the following transcendental equation:

$$z = \tanh (az), \tag{2.31}$$

where $z = (2\rho - 1)$ and $a = N\beta\zeta/2$.

One obvious solution is $\rho = \frac{1}{2}$, which does not correspond to a phase transition. However, if we now plot the curves $f_1(z) = z$ and $f_2(z) = \tanh (az)$ as in Fig. 13, we see that two other solutions are possible corresponding to $z = 2\rho - 1 = \pm z_1$, or

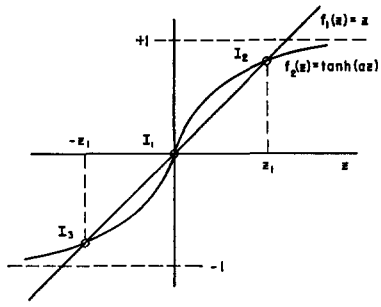

FIG. 13. Graphic solution of Eq. (2.31).

$\rho = \frac{1}{2} \pm x_1$. It is obvious that these additional solutions can exist if and only if the curve $f_2(z)$ has a slope at the origin greater than 1, i.e., if $a > 1$. Hence a phase transition can occur only if $N\beta\zeta > 2$; then ρ is truly a multiple-valued function of the pressure, having the values $\rho = \frac{1}{2} + z_1, \frac{1}{2}$, and $\frac{1}{2} - z_1$, all corresponding to the pressure $p = (kT/l) \lim_{N\to\infty} (1/N) \ln (T_m)$. The critical temperature of the system must therefore be given by the condition $N\beta\zeta = 2$. This, then, confirms the limit of the quantity $N\beta\zeta$ discussed in connection with Table II. We note that in the thermodynamic limit the critical temperature is infinite. For finite systems the preceding conclusions hold only approximately, since in that case T_m is no longer the only significant term. There is then also a contribution from the remainder term. Table III allows a comparison of the "critical" temperatures of finite systems obtained numerically and from the relation $a = 1$ (which, as pointed out, does not hold exactly for such systems). For infinite systems one notes that $\lim_{N\to\infty} a = \infty$ so that from Eq. (2.31) z can only take on the values ± 1; i.e., ρ is restricted to the values zero and one. Consequently the phase transition of this system in the thermodynamic limit is a degenerate one resembling that in Fig. 8.

III. ANALYSIS OF FINITE SYSTEMS

In Sec. II we examined various fluids with interaction potentials that allowed us to go to the thermodynamic limit. This section is devoted to an investigation of systems in which every particle interacts with every other one, i.e., which interact with the full Lennard–Jones potential. In that case we cannot go to the limit $N \to \infty$. However, the series solution of the partition function, Eq. (1.1), is well suited to numerical analysis. Hence we consider systems of finite and in fact quite modest size for which the thermodynamic properties were determined by means of an IBM 360 model-40 computer. Computer time increased very rapidly with system size so that it was not feasible to investigate systems with more than 15 cells. Some caution is in order in speaking of the thermodynamic functions of such systems since we are dealing here with finite assemblies and cannot go to the thermodynamic limit. We shall denote these functions by their usual symbols but interpret them in a common-sense way.

TABLE III. Comparison of critical temperatures for a one-dimensional system with infinite-range interactions.

N	T_c (Numerical)	T_c' (Analytic)[a]	T_c/T_c'
10	193.95	320	0.60
20	438.35	640	0.68
50	1233.76	1600	0.78
100	2637.53	3200	0.82
200	5558.49	6400	0.87
240	6729.81	7680	0.88

[a] The analytically determined temperature T_c' holds exactly only in the thermodynamic limit. For the finite systems considered here it is an approximation.

A. Formulation of the Problem for Numerical Analysis

We define a function T as follows [cf. Eq. (1.1)]:

$$T(\nu, \beta, N) = \sum_{n=0}^{[N/2]} T_n. \tag{3.1}$$

The grand potential is then given by

$$q = \beta p l = \nu + (1/N) \ln (2T). \tag{3.2}$$

The density of the system is

$$\rho = (\tfrac{1}{2})(1 + T_\nu/NT), \tag{3.3}$$

where $T_\nu = (\partial T/\partial \nu)_\beta$. For the compressibility one obtains:

$$K_T = (\beta l/4\rho^2)[T_{\nu\nu}/NT - (2\rho - 1)^2 N], \tag{3.4}$$

where $T_{\nu\nu} = (\partial^2 T/\partial \nu^2)_\beta$. The internal energy density is

$$u = (\tfrac{1}{2})\rho kT + \rho \sum_{r=1}^{N} V_r - T_\beta/NT, \tag{3.5}$$

where $T_\beta = (\partial T/\partial \beta)_\nu$. For the specific heat one finds

$$C_\nu = \tfrac{1}{2}k\rho + k\beta^2[(T_{\beta\beta}/NT) - (1/N)(T_\beta/T)^2] + k\beta^2[(T_{\nu\beta}) - (2\rho - 1)NT_\beta]^2/[NT((2\rho - 1)^2 N^2 T - T_{\nu\nu})], \tag{3.6}$$

where $T_{\beta\beta}$, $T_{\nu\beta}$, etc., have the obvious interpretation.

We next wish to find a pair-correlation function that is amenable to numerical analysis. For this purpose we define an average correlation parameter as follows:

$$S_i = (1/N)\left\langle \sum_{r=1}^{N} \sigma_r \sigma_{r+i} \right\rangle. \tag{3.7}$$

One observes that $S_i = 1$ if cells in the system separated by i cell parameters are either all occupied or all empty. If one cell is occupied while the other is empty for every pair of cells separated by i cell parameters, then perfect anticorrelation exists and $S_i = -1$. Finally, $S_i = 0$ corresponds obviously to a state of no correlation. In order to find the relationship between the correlation parameter defined above and the usual pair correlation functions, we restrict ourselves to the case $\rho = \frac{1}{2}$ since we are principally interested in the order of the system in the transition region. It is shown in Appendix C that this relationship is as follows[8]:

$$S_i = (1/N)\sum_{r=1}^{N} C^{(2)}(\sigma_r, \sigma_{r+i}) - 1, \qquad (3.8)$$

or in terms of the Kirkwood correlation functions, which have found more frequent use in dealing with fluids:

$$S_i = 1/(N-1)\sum_{r=1}^{N} g^{(2)}(\sigma_r, \sigma_{r+i}) - 1. \qquad (3.9)$$

For convenience we shall refer to the correlation parameter S_i simply as correlation function in what follows.

The correlation functions are readily computed from (1.1) by noting that

$$S_i = (\tfrac{1}{2}N)(\partial/\partial\theta_i) \times \ln\left\{\sum_{\{\sigma\}} \exp\left(\sum_{r=1}^{N}\sum_{s=1}^{N}\sigma_r\sigma_{r+s}\theta_s + \nu\sum_{r=1}^{N}\sigma_r\right)\right\} \qquad (3.10)$$

It follows then that:

$$S_i = 1 + (T_{\theta_i}/2NT) \qquad (3.11)$$

where

$$T_{\theta_i} = (\partial T/\partial\theta_i)_v = 8(\partial T/\partial x_i)_v = \sum_{n=0}^{[N/2]} \cosh[(N-2n)\nu]X^{-n/2}\{(t_n)_{\theta_i} - 8n\} \qquad (3.12)$$

and

$$(t_n)_{\theta_i} = (\partial t_n/\partial\theta_i) = (8/n!)\sum_{q_1=1}^{N}{}' \cdots \sum_{q_n=1}^{N}{}' \prod_{r=1}^{n}\prod_{\substack{s=1\\(r<s)}}^{n} x_{(q_r-q_s)}\delta_{(q_r-q_s),i}.$$

(We assume for convenience that N is odd.)

B. Results for One-Dimensional Systems

Specific-heat curves for systems ranging in size from two to fourteen cells are shown in Fig. 14. The curves are for a potential-well depth of $\zeta = 64k$ which corresponds roughly to that of Neon.[12] One observes

[12] W. Band, *An Introduction to Quantum Statistics* (D. Van Nostrand Co., Inc., New York, 1955).

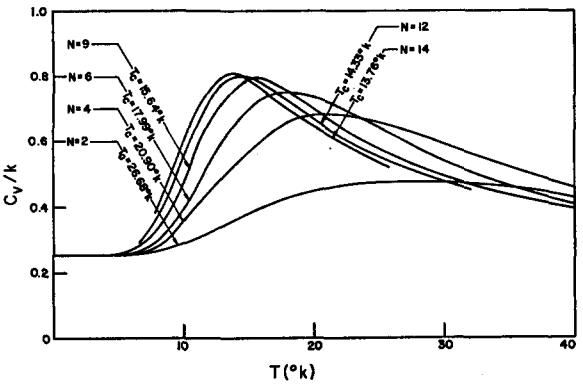

FIG. 14. Specific heat vs temperature for a one-dimensional system; $\zeta = 64k$; $\gamma = 6$; $\rho = \frac{1}{2}$.

that the maxima of these curves becomes higher and steeper with increasing system size and moves toward lower temperatures. Table IV summarizes this information. The term "critical" temperature is used loosely in this table and in what follows to mean the temperature at which the specific-heat curve has a maximum. It is apparent that the specific-heat maxima approach a limit; however, from the information available one cannot say with any certainty what this limit is. If one expands ζ/kT_c in inverse powers of N and fits the expansion parameters to the numerical data, one obtains

$$\zeta/kT_c \simeq 6.43 - 31.16/N + 87.36/N^2. \qquad (3.13)$$

Table IV also shows the values of ζ/kT_c obtained from this equation. The fit is seen to be excellent for systems of six cells or more. If Eq. (3.13) were to remain valid for larger systems one would conclude that $\lim_{N\to\infty} \zeta/kT_c = 6.43$ which, for the neonlike potential used in Fig. 14 would correspond to $T_c \simeq 10°K$.

Specific-heat curves for different potential-well depths are plotted in Fig. 15 for a 12-cell system. The

TABLE IV. Summary of critical data for one-dimensional specific heat curves.

System size (N)	Critical temperature (T_c)	ζ/kT_c True	ζ/kT_c Eq. (3.13)
2	26.68	2.39	12.69
4	20.90	3.06	4.10
6	17.99	3.56	3.66
9	15.64	4.09	4.04
10	15.14	4.22	4.18
11	14.74	4.34	4.32
12	14.33	4.44	4.44
13	14.08	4.55	4.55
14	13.76	4.65	4.65

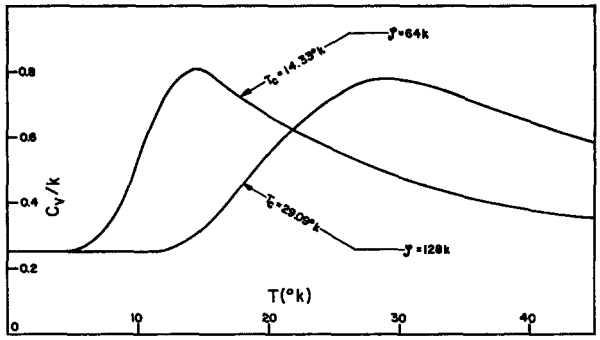

FIG. 15. Specific-heat vs temperature for a one-dimensional system; $N = 12$; various potential-well depths; $\gamma = 6$; $\rho = \frac{1}{2}$.

maxima of these curves occur at higher temperatures as the potential-well depth is increased. Comparable curves for a fixed depth of the potential well but for various range parameters are shown in Fig. 16. It appears from these data that the effect of increasing the effective range of interaction, i.e., of decreasing the parameter γ, is similar to that of increasing the potential-well depth. Both shift the maxima to higher temperatures. One can incorporate the γ and ζ dependence into an equation similar to (3.13)

$$\zeta/kT_c = \alpha_\gamma \exp\{(m-1)/100\} \times [1.53 - 7.42/N + 20.80/N^2], \quad (3.14)$$

where m is given by $\zeta = 2^m k$ and

$$\alpha_\gamma = \gamma - (\gamma-1)(\gamma-2)(\gamma-3)/(18+2\gamma).$$

This equation fits the numerical data with quite good accuracy.

Pressure-vs-density data for systems of various sizes are plotted in Fig. 17. As the size of the system increases, the interaction becomes more effective and the pressure for a given density is reduced. Figure 18 shows the change of the p–ρ isotherms with temperature for a 12-cell system. Pressure is seen to decrease with decreasing temperature as one would expect. There is,

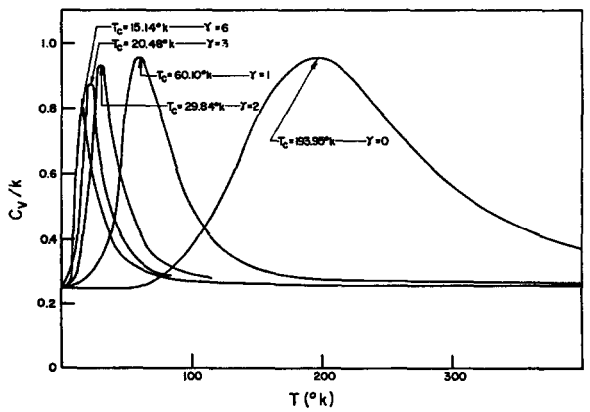

FIG. 16. Specific-heat vs temperature for a one-dimensional system with different potential range parameters; $N = 10$; $\zeta = 64k$; $\rho = \frac{1}{2}$.

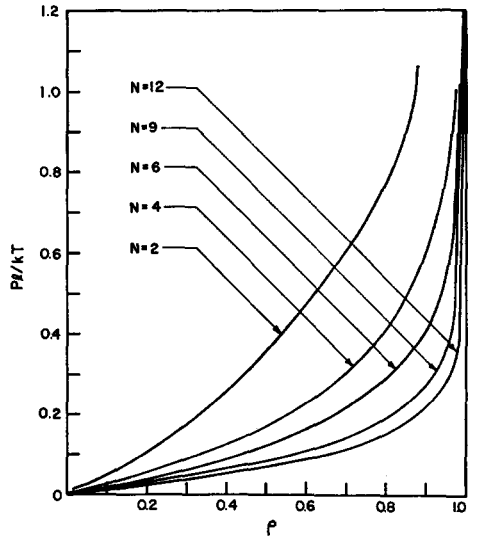

FIG. 17. Pressure-vs-density isotherms for one-dimensional systems of various sizes; $T = 10°\text{K}$; $\zeta = 64k$; $\gamma = 6$.

however, no indication of a phase transition. However, in Fig. 19, which depicts the "critical" isotherms for a 10-cell system with various interaction potentials, we observe a noticeable inflection and flattening of these curves. This is rather reminiscent of the curves in Fig. 11 and could presage a change of phase. Interestingly enough it is found that all critical isotherms fall within the narrow band bordered by the curves marked A and B. This seems to suggest that a law of corresponding states may apply approximately. At the critical density one finds from the upper curve, which coincides with all but two of the isotherms, that $pl/kT_c = \beta_c p_c l = 0.135$. Hence, $\beta_c p_c V_c = \beta_c p_c l/\rho_c = 0.270$. Hill shows in Table II, p. 232, that the mean

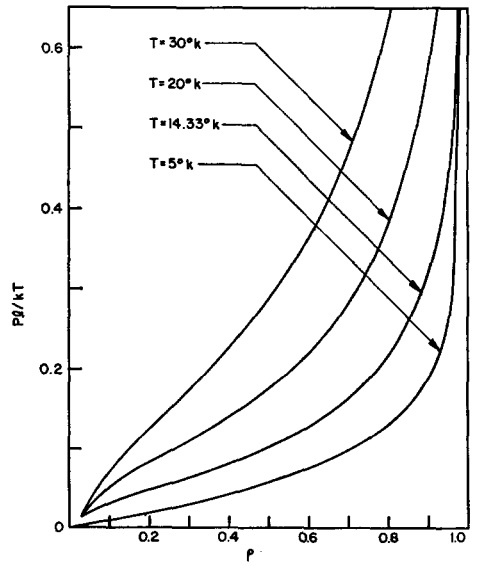

FIG. 18. Pressure-vs-density isotherms for a one-dimensional system; $N = 12$; $\zeta = 64k$; various temperatures.

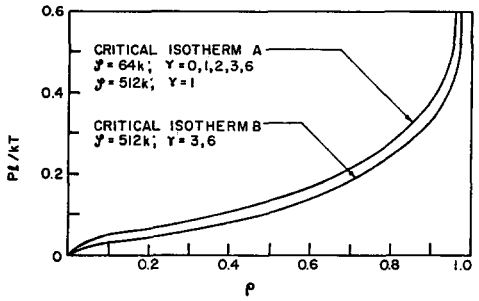

FIG. 19. "Critical" pressure-vs-density isotherms for a one-dimensional system with different interaction potentials; $N = 10$.

value of this parameter for Ne, N_2, A, and CH_4 is 0.292.[8] The potentials plotted in Fig. 19 are approximately those for Ne and A. Consequently the critical value obtained from the present one-dimensional model lies within 7.5% of the experimental value for real three-dimensional fluids.

Compressibility curves for systems of various sizes are plotted in Fig. 20. These are seen to exhibit normal fluid behavior, without any indication of a phase transition. Figure 21, on the other hand, shows compressibility evidencing some rather interesting anomalous behavior. These curves are the analogs of those in Fig. 19 for a potential-well depth of $64k$. The anomalies clearly correspond to the inflections in

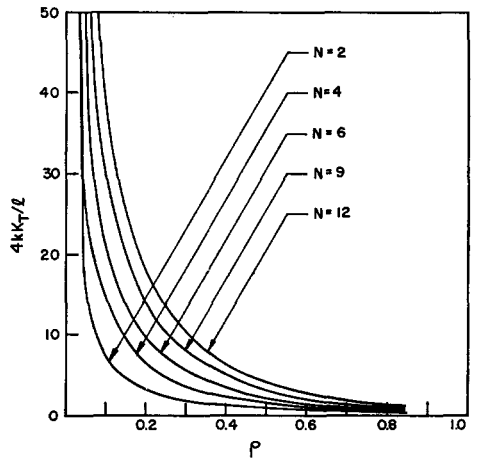

FIG. 20. Compressibility vs density for one-dimensional systems of various sizes; $T = 10°K$; $\zeta = 64k$; $\gamma = 6$.

ranging in size from 5 to 15 cells are plotted in Fig. 23 for a temperature of 32°K and a density of $\rho = \frac{1}{2}$. These are seen to agree quite well qualitatively with experimental curves and curves for radial distribution functions computed by other methods.[8,13,14] Correlation is largest for nearest neighbors, then drops off and approaches zero. However, one observes an absence of the local maxima and minima that are usually so characteristic of these curves. The difference in behav-

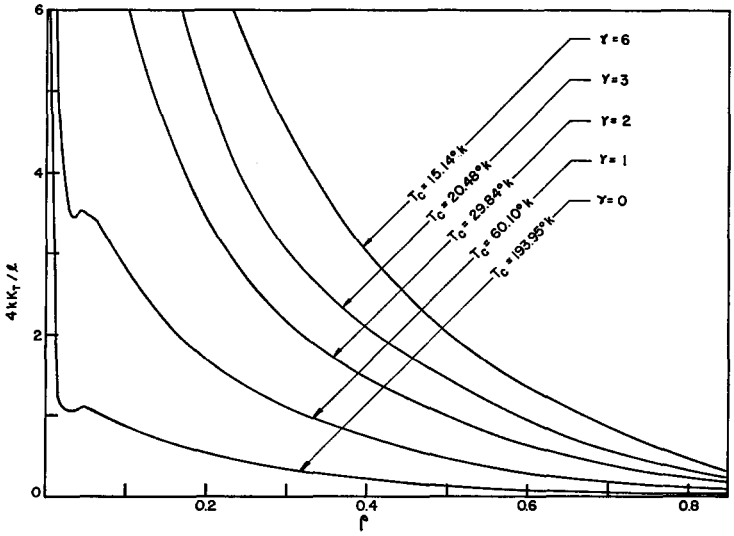

FIG. 21. Compressibility vs density for a one-dimensional system with various potential ranges; $N = 10$; $\zeta = 64k$.

slope in Fig. 19 and may be associated with an incipient phase transition. This behavior appears even more clearly in Fig. 22, where pressure and compressibility isotherms are plotted on the same graph. Both are for a 12-cell system at its "critical" temperature. The inflection in the p–ρ curve and the corresponding anomaly in the compressibility curve are plainly visible.

The pair-correlation functions for selected systems

ior appears to be due to the discrete nature of the cellular model used here. De Boer has shown that the undulations are due to contributions to the potential of average force from the screening effect of particles

[13] S. Fluegge, *Handbuch der Physik, Vol. XIII*, (Springer Verlag, Berlin, 1962).

[14] J. O. Hirschfelder, C. F. Curtiss, and R. B. Bird, *Molecular Theory of Gases and Liquids* (John Wiley & Sons, Inc., New York, 1954).

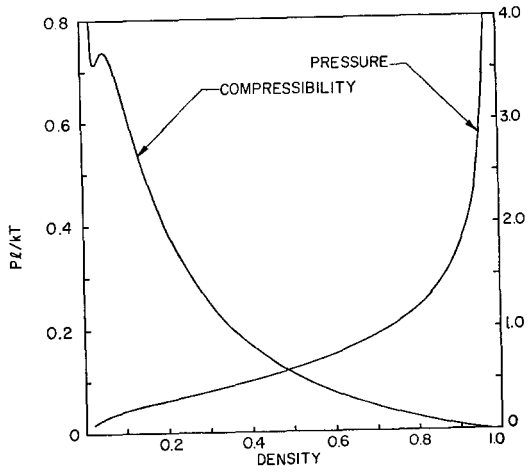

FIG. 22. Pressure and compressibility vs density for a 12-cell one-dimensional system; $T = 14.33°\text{K}$; $\zeta = 64k$.

surrounding the particle of interest.[15] The effect, according to de Boer, is to superpose an extra repulsive force at distances smaller than $1.5l$, an extra attractive force between $1.5l$ and $2.2l$, and a small repulsive force at larger distances. In the present model all potentials are averaged over the whole cell. Thus the variations discussed by de Boer are smeared out over the entire cell and are more than compensated for by the attractive Lennard–Jones potential. In Fig. 24 we see the effect of temperature on correlation for a 13-cell system. At temperatures well below the critical point one sees that correlation is perfect, or very nearly so,

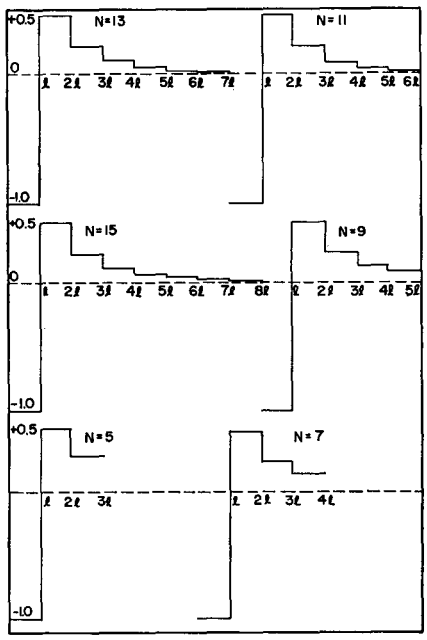

FIG. 23. Pair-correlation functions for one-dimensional systems of various sizes; $T = 32°\text{K}$; $\zeta = 64k$; $\gamma = 6$; $\rho = \frac{1}{2}$.

[15] J. de Boer, Rept. Progr. Theoret. Phys. (Kyoto) **12**, 305 (1949).

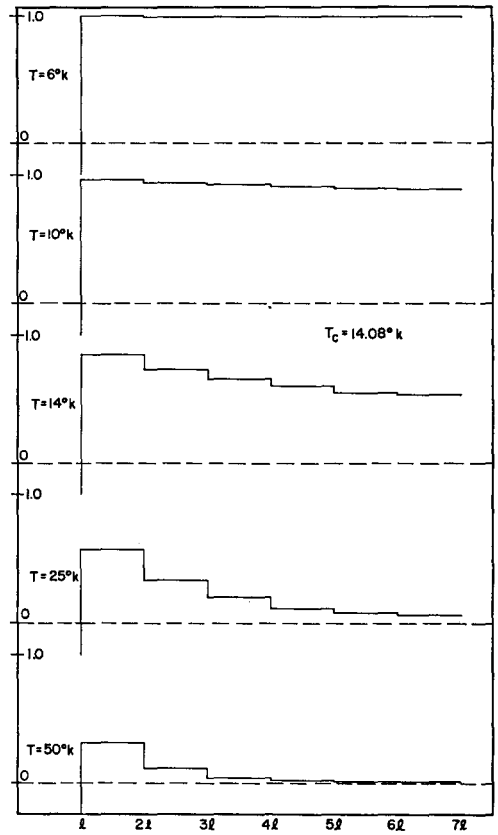

FIG. 24. Pair-correlation functions for a 13-cell system at various temperatures; $\zeta = 64k$; $\gamma = 6$; $\rho = \frac{1}{2}$.

throughout the entire system. Long-range order exists. As the temperature increases, correlation is gradually reduced, less so for nearest-neighbor cells and more for cells far removed from one another. Long-range order changes to short-range order. The drop in correlation is particularly marked for temperatures higher than the critical one. This is shown more

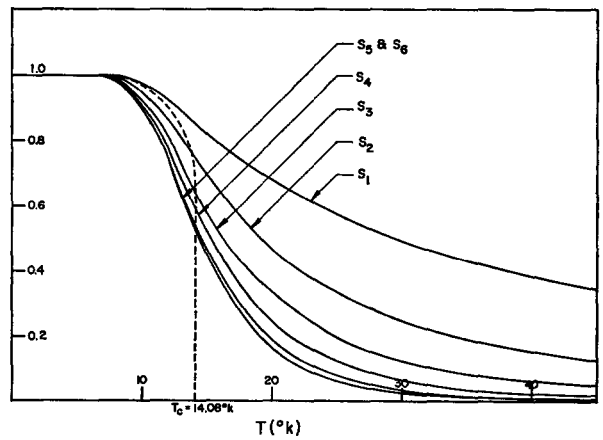

FIG. 25. Pair-correlation functions vs temperature for a 13-cell system; $\zeta = 64k$; $\gamma = 6$; $\rho = \frac{1}{2}$.

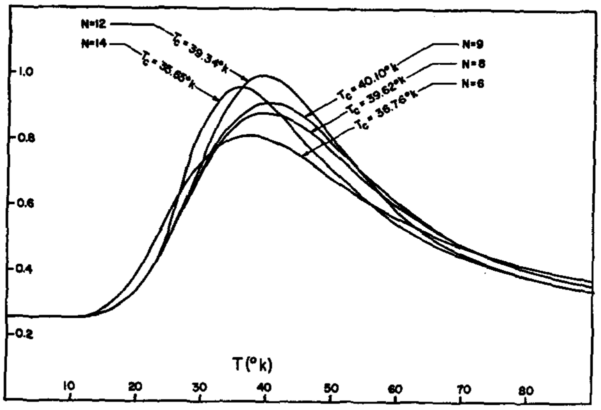

FIG. 26. Specific heat vs temperature for typical two-dimensional systems; $\zeta = 64k$; $\rho = \frac{1}{2}$.

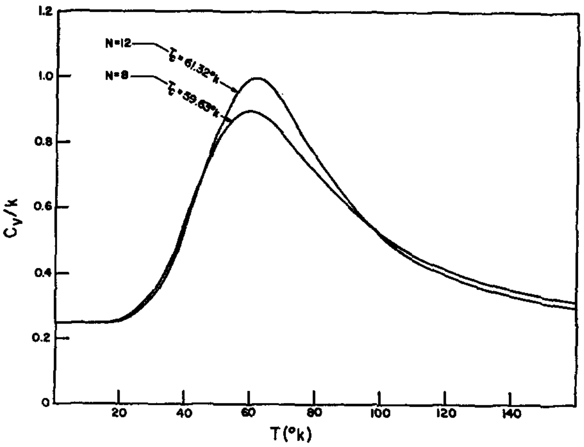

FIG. 27. Specific heat vs temperature for two typical three-dimensional systems; $\zeta = 64k$; $\rho = \frac{1}{2}$.

clearly in Fig. 25 where the correlation functions for this same system are plotted against temperature. We see that nearest-neighbor correlation decreases only slowly; however, the longer-range correlations drop off markedly as the critical temperature is approached and passed. The graph shows very clearly how long-range order changes to short-range order at the "critical" temperature. The behavior is completely analogous to that found by Kaufman and Onsager in their investigation of the two-dimensional Ising ferromagnet.[16] Since in the two-dimensional Ising model this behavior is associated with a phase transition, one surmises that in the present instance it might be indicative of an incipient change of phase. The surmise is reinforced by the behavior discussed in connection with Fig. 22.

C. Results for Two- and Three-Dimensional Systems

Section 2B and 6B of Paper I dealt with application of the present model to multi-dimensional systems. In this section we present some results for small two- and three-dimensional systems with nearest-neighbor interactions only that were obtained by computer. The potential used was:

$$V_s = \begin{cases} -64k & (s=1,m) \quad (s=1,m,k) \\ 0 & (s\neq 1,m) \quad (s\neq 1,m,k) \end{cases} \text{Mod. } N. \tag{3.15}$$

(first column: *two-dimensional system*; second column: *three-dimensional system*)

Two-dimensional systems accessible within the restriction $N \leq 15$ are those having 4, 6, 8, 9, 10, 12, 14, and 15 cells, respectively, while three-dimensional systems are confined to $N = 8$ and 12.

[16] B. Kaufman and L. Onsager, Phys. Rev. 76, 1244 (1949).

Specific-heat curves for typical two- and three-dimensional fluids are shown in Figs. 26 and 27, respectively. As in the one-dimensional case, the curves exhibit a characteristic peak which is shifted to higher temperatures with increasing dimensionality of the system. Table V summarizes the "critical" temperature data available for these systems. For the two-dimensional system the exact value for the ratio ζ/kT_c is 1.76.[17] It is seen that the values in Table V

TABLE V. "Critical" temperature data for two- and three-dimensional systems for $\zeta = 64k$, $\rho = \frac{1}{2}$.

System size (N)	"Critical" temperature (T_c) 2-Dim. system	3-Dim. system	ζ/kT_c 2-Dim. system	3-Dim. system
6	36.76	—	1.74	—
8	39.62	59.63	1.61	1.07
9	40.10	—	1.59	—
12	39.34	61.32	1.62	1.04
14	35.65	—	1.79	—

fluctuate about the exact ratio within approximately ±10%. These fluctuations are attributable to the small size of the systems investigated, the differences in symmetry of the systems, and the consequent strong influence of boundary effects (spurious interactions). (The 14-cell system, for example, consists of two rows of seven cells each, while the 12-cell one has three rows of four cells. There are thus obvious differences in symmetry.) For the three-dimensional system, Wakefield's value of the corresponding ratio is generally considered the most accurate[13]:

$$\exp\{-2J/kT_c\} = 0.641.$$

[17] L. Onsager, Phys. Rev. 65, 117 (1944).

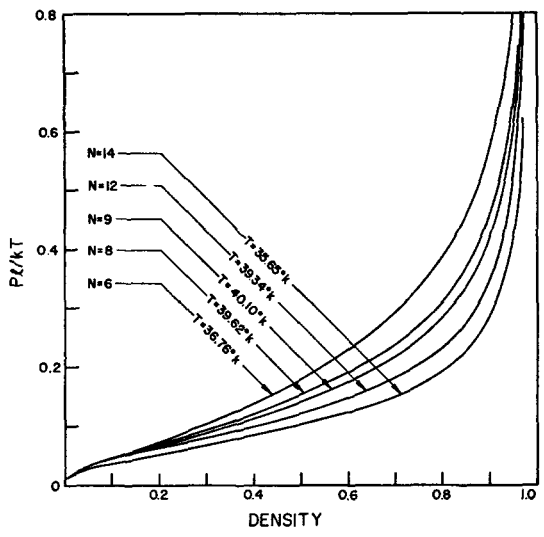

FIG. 28. Pressure vs density, two-dimensional systems; $\zeta = 64k$; $T = T_c$.

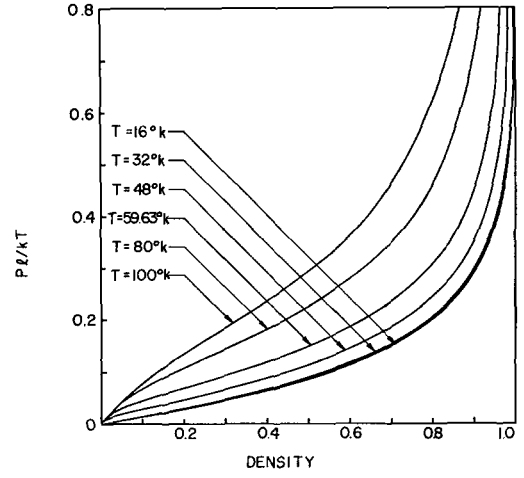

FIG. 30. Pressure–density curves for an eight-cell three-dimensional system; $\zeta = 64k$.

In terms of the parameters of the present model this is equivalent to $\zeta/kT_c = 1.05$. (ξ for the nearest-neighbor fluid corresponds to $4J$ for the ferromagnet.) Other estimates of this ratio range from 0.98 to 1.09.[13] The values obtained from the model considered here fall well within this range and differ from the best value by less than 2%. This accuracy is most likely due to the perfect and almost perfect cubic symmetry of these two systems. It is nonetheless remarkable that such close agreement should be obtained for assemblies of so small a size.

Pressure-vs-density graphs for typical two- and three-dimensional systems are shown in Figs. 28 through 30. They exhibit normal fluid behavior except that there is, of course, no phase transition. Lowering the temperature and increasing the system size are both seen to lower the pressure for a given density. In addition, one observes again the rather characteristic inflection of the isotherms. The compressibility curves for the 9-cell two-dimensional system in Fig. 31 correspond to the p–ρ curves in Fig. 29. One clearly discerns anomalous behavior in these curves at temperatures below the "critical" one. This same behavior and the correlation between the inflection of the p–ρ curve on the one hand and the corresponding inversion of the K_T–ρ curve on the other is shown even more clearly in Fig. 32, where these two curves for a 12-cell three-dimensional fluid have been super-

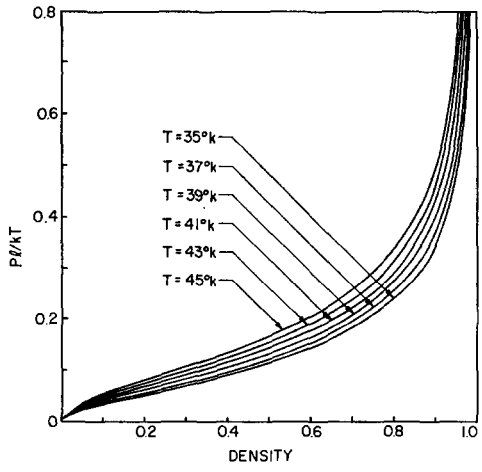

FIG. 29. Pressure–density curves for a nine-cell two-dimensional system, various temperatures; $\zeta = 64k$.

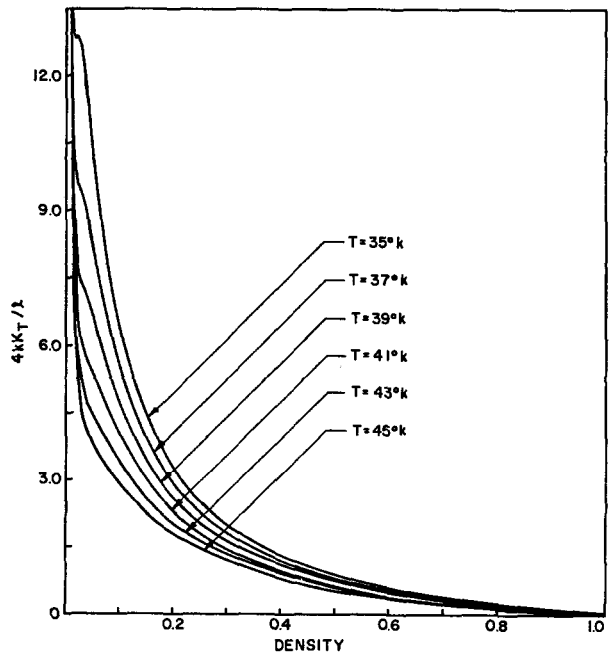

FIG. 31. Compressibility-vs-density isotherms for a nine-cell two-dimensional system; $\zeta = 64k$.

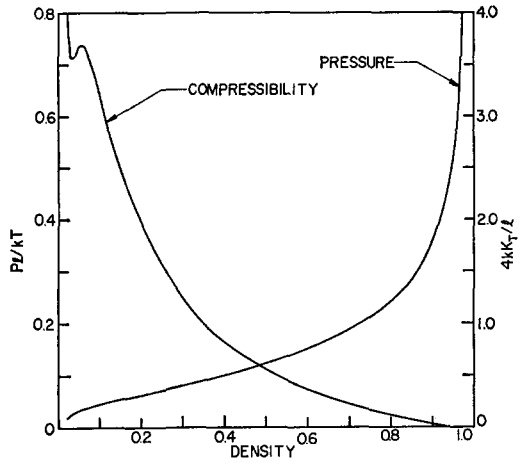

FIG. 32. Pressure-and-compressibility-vs-density isotherms for a 12-cell three-dimensional system.

posed on the same graph. Since we know that two- and three-dimensional systems in the thermodynamic limit are subject to phase transitions, one surmises that this behavior in the pressure-and-compressibility isotherms is indicative of an incipient transition. The analysis in Sec. II.D and in particular Figs. 11 and 12 lend further credence to this surmise.

IV. CONCLUSIONS

The fluid model examined in this series of two articles was seen to combine mathematical convenience with considerable flexibility. Despite its simplicity it proved capable of yielding realistic and consistent thermodynamic results and of portraying phase transitions correctly. In I it was found that the introduction of a cellular structure made an otherwise difficult problem mathematically much more tractable. The price paid for this simplification was an uncertainty in the instantaneous locations of the particles comprising the system. One could only say that a given particle is located within a certain cell with an uncertainty proportional to the cell parameter. By keeping the cell size small and in fact letting it coincide with the particle's exclusion sphere it was possible to keep this uncertainty within reasonable bounds. The model then represents an approximation to real physical systems but is not exactly equivalent to any such system. This is not the only approximation incorporated in the model. Others include the assumption that the system can be treated classically, the restriction of the configurational energy to pairwise interactions, the adoption of the Lennard–Jones potential with hard-core cutoff for the interaction energy, etc. These latter approximations are fairly standard, however, in theoretical investigations of this type and appear to be quite reasonable for simple nonquantum fluids such as the inert gases. The discrete cellular structure also does not seem to affect the thermodynamic behavior of the model too adversely. In any event, qualitative agreement with the behavior of real fluids is seen to be quite good and even phase transitions can be reproduced in a qualitatively correct manner. Since the basic model investigated here is a one-dimensional one, qualitative agreement is perhaps all that can be expected. Nonetheless, on occasions we found quantitative agreement as well. The critical ratio $\beta_c p_c v_c$ mentioned in Sec. II is a case in point. Such agreement may, of course, be fortuitous.

Despite the relative mathematical simplicity of the model it is surprisingly versatile. We noted this in I already, where we saw how the basic one-dimensional system in which all particles interact with one another can be converted into a two- or three-dimensional one with more limited interactions. It proved possible by virtue of this transformation to obtain series expansions in all dimensions by an identical straight-forward algebraic method. Also, we noted there that the model offers a convenient method for investigating the zeros of the partition function, thereby providing further insight into the analyticity of that function and therefore into the nature of the phase transitions to which it may give rise. Current research is being focused on this area.

In the present article we have explored this versatility of the model further by applying it to various types of systems in order to investigate their thermodynamic behavior. Thus we saw that the model correctly and almost trivially yields the equation of state of an ideal gas and of a Tonks gas in the limit of no interaction and of only a hard-core interaction, respectively. This provided further evidence of the validity of the model, at least in that limit, over and above the analysis in I. The one-dimensional fluid with nearest-neighbor interactions, which was investigated next, offered the unique advantage that the equation of state and all thermodynamic functions can be written in closed form. This system consequently offers a mathematically very tractable model for investigating thermodynamic behavior in a fluid having attractive interactions of limited range combined with a hard repulsive core. Obvious limitations of the system are its one-dimensional nature and the consequent (by virtue of Van Hove's theorem) absence of a phase transition. Nonetheless the behavior of this system turns out to be surprisingly realistic in many ways.

If one is primarily concerned with phase transitions, the one-dimensional fluid with attractive forces of infinite range (i.e., where $\gamma \to 0$) provides an interest-

ing test case. While physically this obviously does not correspond to any real system, it represents an interesting limit exhibiting typical transition behavior. Investigation of finite systems of this type showed how a phase transition is approached gradually with increasing system size without need for recourse to a Maxwell-type construction. In a 240-cell system the pressure–density isotherm is practically indistinguishable from that of a fluid undergoing a true phase transition, while the compressibility curve shows a very realistic approach to a true discontinuity. Exact analysis confirms the numerical results and indicates that in the thermodynamic limit this fluid has an infinite critical temperature.

In investigating finite one-, two-, and three-dimensional systems of quite modest size the series solution of the partition function used in this study proved quite convenient for computer analysis. It was found that small one-dimensional fluid systems interacting with the full Lennard–Jones potential exhibit many of the characteristics of real fluids. There is, however, no phase transition for systems of so small a size. Nevertheless several indicators suggest that if one could investigate larger systems one would see an approach to a phase transition just as one did in the case of the infinite-range fluid:

(1) The maxima of the specific-heat curves seem to approach a limiting critical temperature, other than absolute zero, and also approach a typical shape.

(2) The pressure–density isotherms begin to show a typical inflection that is usually associated with systems approaching a phase transition. The compressibility isotherms display a corresponding inversion which could well presage an approach to a discontinuity.

(3) Analysis of pair-correlation functions with respect to temperature shows quite conclusively that long-range order prevails at low temperatures and changes quite abruptly to short-range order as the "critical" temperature of the system is passed.

Analysis of small two- and three-dimensional systems with nearest-neighbor attractive interactions indicates that the "critical" temperatures obtained from their specific-heat maxima agree within a few percent with those obtained by other methods in the thermodynamic limit. The excellent agreement achieved is rather surprising in view of the very small size of the systems investigated here and the consequently quite pronounced effect of spurious interactions. These systems exhibit the same behavior in the pressure-and-compressibility isotherms as that mentioned in (2) above. Since we know from other evidence that two- and three-dimensional systems in the thermodynamic limit are subject to phase transitions, one can by analogy construe this analogous behavior of the pressure-and-compressibility isotherms as further indication of a possible approach to a phase transition in the one-dimensional case.

The model investigated in this study appears quite promising and worthy of further examination. It would be of particular interest to investigate the general one-dimensional system with all interactions active in the thermodynamic limit. To that end one must either aim at finding a closed-form solution or a valid approximation. Alternatively one should try to extend computer analysis to very much larger systems. These approaches are currently being investigated. Other present research is concerned with critical exponents and it is hoped that some results concerning these will be available in the near future.

ACKNOWLEDGMENTS

One of the authors (R. G. T.) is greatly indebted to the Physics Department, University of Missouri at Rolla, for partial support of this research and to Professor R. E. Lee and his staff for valuable assistance and for so generously making available computer time and the facilities of the UMR Computer Center.

APPENDIX A: THE HARD-CORE POTENTIAL AND CELL PARAMETER

We first wish to show the connection between the hard-core potential and the primed sums that occur in the series solution, Eq. (1.1) of this article or Eq. (4.7) of I. Let us temporarily revoke the convention adopted in I for mathematical convenience that $V_0 = \phi_0 = 0$ (Mod. N). Instead we write the potential explicitly as follows:

$$\eta_s = \begin{Bmatrix} \zeta_{hc} & (s = 0) \\ -\zeta/s^\nu & (s \neq 0) \end{Bmatrix} \quad \text{(Mod. } N\text{)}. \qquad \text{(A1)}$$

where $\zeta_{hc} = +\infty$ is the hard-core potential. The corresponding Boltzmann factor is

$$z_s = \exp\{-\beta\eta_s\} = \begin{Bmatrix} \exp(-\beta\zeta_{hc}) & (s = 0) \\ \exp(\beta\zeta/s^\nu) & (s \neq 0) \end{Bmatrix} \quad \text{(Mod. } N\text{)}. \qquad \text{(A2)}$$

The hard-core part of z_s can be written as $(1 - \delta_{s,0})$ so that the entire Boltzmann factor becomes:

$$z_s = (1 - \delta_{s,0}) \exp(\beta V_s)$$
$$V_s = \begin{cases} 0 & (s = 0) \\ -\zeta/s^\nu & (s \neq 0). \end{cases} \qquad \text{(A3)}$$

It will be observed that V_s is the potential of Paper I with the convention $V_s = \phi_s = 0$, which is seen to arise naturally in this way. Consider now the primed

sums in Eq. (1.1)

$$t_n = (1/n!)\sum_{q_1=1}^{N}{}' \cdots \sum_{q_n=1}^{N}{}' \prod_{\substack{r=1\\(r<s)}}^{n}\prod_{s=1}^{n} x_{(q_r-q_s)}. \quad \text{(A4)}$$

The primes imply that no index may be repeated in any given term of the sum. Hence one can also write

$$t_n = (1/n!)\sum_{q_1=1}^{N} \cdots \sum_{q_n=1}^{N} \prod_{\substack{r=1\\(r<s)}}^{n}\prod_{s=1}^{n}(1-\delta_{(q_r-q_s)})x_{(q_r-q_s)}$$
$$= (1/n!)\sum_{q_1=1}^{N} \cdots \sum_{q_n=1}^{N} \prod_{\substack{r=1\\(r<s)}}^{n}\prod_{s=1}^{n} z_{(q_r-q_s)}, \quad \text{(A5)}$$

where the sums in (A5) are now unrestricted and where Eq. (A3) was used. Thus the primed summations arise from the hard-core repulsive potential and incorporate the exclusion principle that has been built into the model. The expansion of these primed sums is given, for the first few terms, in Sec. 6 of I.

Next, we wish to clarify the relationship that exists between the cell parameter l and the hard-core repulsive potential. Let d be the diameter of the particle's exclusion sphere (the particle's exclusion length in one dimension). Suppose we choose a cell parameter such that $l_0 < d$. Then each particle occupies $-[-d/l_0] = m'$ cells, where [ ] means "nearest integer equal to or less than." The entire system has $L/l_0 = k$ cells where $k > N$, N being given by L/l and l is the usual cell parameter used in this study ($l = d$). Assuming for convenience that m is odd, we define $m = (\frac{1}{2})(m' - 1)$. The appropriate true potential is now given by (A2). In view of the change in cell dimension we must rewrite Eq. (A3) as follows:

$$z_s = (1 - \delta_{s,0} - \delta_{s,1} - \cdots - \delta_{s,m} - \delta_{s,N-1} - \cdots - \delta_{s,N-m}) \exp(\beta v_s). \quad \text{(A6)}$$

Upon introducing this Boltzmann factor into the expression for t_n one finds that one can write

$$t_n = (1/n!)\sum_{q_1=1}^{k} \cdots \sum_{q_n=1}^{k} \prod_{\substack{r=1\\(r<s)}}^{n}\prod_{s=1}^{n}(1-m'\delta_{(q_r-q_s)})x_{(q_r-q_s)}, \quad \text{(A7)}$$

for a fluid of hard rods $x_s = 1$, so that one has:

$$t_n(x_s = 1, \forall s) = (1/n!)k(k-m') \times (k-2m') \cdots (k-(n-1)m'). \quad \text{(A8)}$$

Letting now $k = Nm'$ (we shall choose l_0 such that N is an integer), we find $t_n = \binom{N}{n}(m')^n$ and the partition function is:

$$Q_k = \sum_{n=0}^{k}\binom{N}{n}(m')^n y^n = \sum_{n=0}^{m'N}\binom{N}{n}\eta^n \quad \text{(A9)}$$

where $y = \exp(2\nu)$ and $\eta = m'y$. Observing that $\binom{N}{n} = 0$ for $n > N$, we obtain:

$$Q_k = \sum_{n=0}^{m'N}\binom{N}{n}\eta^n = (1+\eta)^N = [1 + (m'l_0/\lambda)\xi]^N$$
$$= (1 + l\xi/\lambda)^N = Q_N. \quad \text{(A10)}$$

This is the same as Eq. (2.1) and shows that choosing the cell parameter smaller than the particle's exclusion length is a trivial variation of the choice adopted in this study. It was pointed out in I that a choice of $l > d$ would not be useful in the present context.

APPENDIX B: COMPUTATION OF THE INTERNAL ENERGY DENSITY BY A DIFFERENT METHOD FOR THE ONE-DIMENSIONAL FLUID WITH NEAREST-NEIGHBOR INTERACTIONS

The following analysis serves to check the validity and meaning of Eq. (2.10). Obviously the first term in this equation is the kinetic contribution and reflects the one degree of freedom of the system. It requires no further analysis. To proceed with the other terms we define the following quantities:

N_+ = Expected number of occupied cells = $\langle n \rangle$.
N_- = Expected number of empty cells = $N - \langle n \rangle$.
N_{++} = Expected number of nearest-neighbor cells with both cells occupied.
N_{--} = Expected number of nearest-neighbor cells with both cells empty.
N_{+-} = Expected number of nearest-neighbor cells with one cell occupied and one empty.

The following relations are easily seen to hold between these quantities:

$$2N_{++} + N_{+-} = 2N_+$$
$$2N_{--} + N_{+-} = 2N_- \quad \text{(B1)}$$
$$N_{++} + N_{--} + N_{+-} = N.$$

Let us define a parameter (short-range order parameter) σ as follows:

$$\sigma = (1/N)\left\langle \sum_{r=1}^{N}\sigma_r\sigma_{r+1}\right\rangle = (1/N)(N_{++} + N_{--} - N_{+-})$$
$$= 1 - N_{+-}/N = 1 + 4\eta - 4\rho, \quad \text{(B2)}$$

where $\eta = N_{++}/N$. One can determine σ from the partition function as follows [see Eq. (2.10) of I]:

$$\sigma = A_N/N \sum_{\{\sigma\}}\left\{\sum_{r=1}^{N}\sigma_r\sigma_{r+1} \times \exp\left[\epsilon\sum_{s=1}^{N}\sigma_s\sigma_{s+1} + \nu\sum_{s=1}^{N}\sigma_s\right]\right\}\Big/ Q_N$$
$$= (1/N)[(\partial/\partial\epsilon)\ln \Xi_N]_\nu, \quad \text{(B3)}$$

where $\epsilon = \theta_1 = (\frac{1}{4})\beta\zeta$ and $\Xi_N = A_N^{-1}Q_N$. We have

then, using (2.7),

$$\sigma = (\partial/\partial\epsilon)\{\epsilon + \ln(\cosh\nu) + \ln[1 + (1+\omega)^{\frac{1}{2}}]\}_\nu$$
$$= 1 - [2x_1^{-1}\operatorname{sech}^2\nu]/[1 + \omega + (1+\omega)^{\frac{1}{2}}]. \quad \text{(B4)}$$

For the configurational energy of the system we have:

$$U_c = (\tfrac{1}{4})\left\langle \sum_{r=1}^{N}\sum_{s=1}^{N}(1+\sigma_r)(1+\sigma_{r+s})\right\rangle\phi_s, \quad \text{(B5)}$$

where $\phi_s = -(\zeta/2)(\delta_{s,1} + \delta_{s,N-1})$. Carrying out the summations indicated one obtains

$$U_c = -\zeta[(N/4) + (N/2)(2\rho - 1) + (N/4)\sigma], \quad \text{(B6)}$$

so that, using (B4), we have

$$u_c = U_c/N$$
$$= -\zeta\{\rho - [x_1^{-1}\operatorname{sech}^2\nu]/2[1 + \omega + (1+\omega)^{\frac{1}{2}}]\}. \quad \text{(B7)}$$

This is exactly the configurational part of (2.10). By means of (B1) and (B2) one notes that (B6) can be rewritten

$$U_c = -N(\rho - \tfrac{1}{4} + \tfrac{1}{4}\sigma)\zeta = -\zeta N\eta = -\zeta N_{++}. \quad \text{(B8)}$$

This represents just the interaction of all nearest-neighbor occupied cells, as one would expect on physical grounds.

APPENDIX C: RELATIONSHIP BETWEEN VARIOUS CORRELATION FUNCTIONS

We wish to establish the relationship between the correlation parameter used in this study and defined in (3.7) on the one hand and the usual pair-correlation functions. Attention is confined to the case $\rho = \frac{1}{2}$ for reasons indicated following Eq. (3.7). The *a priori* probability that a cell is occupied or empty is $\frac{1}{2}$. The joint probability that cells i and j have occupation indices σ_i and σ_j, respectively is

$$W(\sigma_i, \sigma_j) = W(\sigma_j)W(\sigma_i/\sigma_j) = (\tfrac{1}{2})W(\sigma_i/\sigma_j), \quad \text{(C1)}$$

where $W(\sigma_i/\sigma_j)$ is the conditional probability that cell i has occupation index σ_i given that cell j has occupation index σ_j. Let us suppose that we can write this conditional probability in the form

$$W(\sigma_i/\sigma_j) = W(\sigma_i)(1 + M_{ij}) = (\tfrac{1}{2})(1 + M_{ij}). \quad \text{(C2)}$$

Then

$$W(\sigma_i, \sigma_j) = (\tfrac{1}{4})(1 + M_{ij}). \quad \text{(C3)}$$

Now, given that cell j has occupation index σ_j, the probability that cell i has the same occupation index and the probability that it has the opposite index are mutually exclusive events. Consequently,

$\langle\sigma_i\sigma_j\rangle$ = (probability that cells i and j have the same occupation index) $(+1)$ + (probability that cells i and j have opposite indices) (-1)

$$= M_{ij},$$

and so

$$W(\sigma_i, \sigma_j) = (\tfrac{1}{4})(1 + \langle\sigma_i\sigma_j\rangle). \quad \text{(C5)}$$

We can therefore write the correlation parameter in the following form, with the help of Eqs. (3.7) and (C5)

$$S_i = (4/N)\sum_{r=1}^{N} W(\sigma_r, \sigma_{r+i}) - 1. \quad \text{(C6)}$$

One readily verifies that this equation yields the correct limiting values of $+1$, -1, and 0 for perfect correlation, perfect anticorrelation, and no correlation respectively.

In terms of the usual pair-correlation function, defined as follows:

$$W(\sigma_i, \sigma_j) = W(\sigma_i)W(\sigma_j)C^{(2)}(\sigma_i, \sigma_j)$$
$$= (\tfrac{1}{4})C^{(2)}(\sigma_i, \sigma_j); \quad \text{(C7)}$$

we can write the correlation parameter in the following form[8]:

$$S_i = (1/N)\sum_{r=1}^{N} C^{(2)}(\sigma_r, \sigma_{r+i}) - 1. \quad \text{(C8)}$$

Or, in terms of the Kirkwood correlation functions[8]:

$$S_i = 1/(N-1)\sum_{r=1}^{N} g^{(2)}(\sigma_r, \sigma_{r+i}) - 1. \quad \text{(C9)}$$